Modeling and Simulation of Pedestal Control Technique for NSTX-U

A. Fil, E. Kolemen, N. Ferraro[2], S. Jardin[2], P.B. Parks[1], R. Lunsford[2], R. Maingi[2]

Princeton University, NJ 08540, USA
[1]General Atomics, PO Box 85608, San Diego, CA 92186, USA
[2]Princeton Plasma Physics Laboratory, Princeton, NJ 08543, USA

E-mail contact of main author: afil@princeton.edu

Abstract. In this paper we present initial simulations of pedestal control by Lithium Granule Injection (LGI) in NSTX. A model for small granule ablation has been implemented in the M3D-C1 code [1], allowing the simulation of realistic Lithium granule injections. 2D simulations of Li injections in NSTX H-mode plasmas are done and the effect of granule size, injection angle and velocity on the pedestal gradient increase is studied. The amplitude of the local pressure perturbation caused by the granules is highly dependent on the solid granule size. In our simulations, reducing the granule injection velocity allows one to inject more particles at the pedestal top. First 3D simulations show the destabilization of high order MHD modes whose amplitude is directly linked the granule toroidal localization.

1. Introduction

Real-time pedestal control is a crucial topic for future fusion reactors and ITER where the pedestal has to be kept free of Edge-Localized-Modes (or ELMs) for heat flux management, while maintaining high plasma performance. Many different control schemes have been developed and tested to adjust and regulate the pedestal at NSTX and other devices. NSTX-U is now operational and is planning additional tests. All these techniques aim at changing the pedestal parameters to mitigate ELMs. In particular, gas puffing [2] injects fuel or impurities at the plasma edge to control the plasma pedestal density, 3D magnetic perturbations [3] create an edge stochastic layer increasing the transport (which lowers the pedestal pressure gradient), Lithium Granule Injections (LGI) [4] induce pressure perturbations triggering ELMs and can thus change the ELM frequency and their impact on the Plasma Facing Components (PFCs). The final aim of this work is to combine these methods into an adaptive and automatic pedestal control algorithm for tokamaks. Such a capability could allow one to explore new innovative scenarios such as the Super H-Mode [5] or lithium induced ELM-free regimes [6]. In order to reach this goal, it is important to understand the physics bases for how the different control actuators affect the pedestal. This is especially important in order to evaluate applicability to future reactors, e.g. ITER.

In this paper, we focus on the LGI technique and present numerical simulations of granule induced perturbations to the discharge edge with the M3D-C^1 code. M3D-C^1 [1] is a state-of-the-art 3D full-MHD code with realistic geometry and is being developed to study plasma response when several actuators are triggered (gas puffing, 3D magnetic perturbations and LGI). Experimentally, high frequency Li granule injections have been performed in DIII-D plasmas [7] and a LGI system has recently been installed on NSTX-U. As it is using non-fuel, non-recycling materials, LGI allows a decoupling of ELM control from plasma fueling. DIII-D experiments have demonstrated a robust ELM-pacing and a triggering efficiency higher than 80% for 0.9 mm lithium granules, but some concern exists because of the variability of triggered-ELM sizes. In particular, in high density, low-torque ITER baseline scenarios, an increase of the ELM frequency by LGI-pacing did not directly translate in ELM size mitigation [8]. Modeling with M3D-C^1 has the potential to investigate these phenomena by simulating the non-linear, 3 dimensional dynamic evolution of a realistic tokamak equilibrium subject to a triggered ELM. In this paper, we first present the implementation of granule ablation models in M3D-C[1]. We will then present the results of 2D NSTX LGI simulations that investigate the pressure perturbation triggered by different granule sizes, injection angle and velocity. Finally, we will present first 3D simulations investigating the LGI-triggered MHD.

2. Modeling of lithium granule injection in M3D-C[1]

Two models have been implemented in M3D-C[1] to calculate the ablation rate of the Lithium granule. The first one [9] [10] is a Neutral Gas Shielding Model calibrated on DIII-D experimental measurements of the Lithium granule ablation rates. The second one [11] is valid for small size granules (sub-mm) where the contribution of plasma ions to the granule ablation is not negligible. In both cases, the granule is modeled as a varying density source that is a Gaussian multiplied by the normalized ablation rate A_r. The width of the source is defined by the realistic granule radius r_p multiplied by an arbitrary parameter. This parameter allows a modification of the size of the ablation cloud experimentally observed around the granule. Note that this is the only ”free” parameter of the granule model and that experimentally its value is imprecise (between 5-100 times the solid granule radius). Its impact on the simulations will be discussed in section 3.
The granule ablation rate is calculated at each time-step as $A_r = C\ (n_e, T_e, r_p) \times X_m$, where r_p is the granule radius and (n_e, T_e) are the electron density and temperature of the background plasma at the granule position. $C\ (n_e, T_e, r_p)$, the non-dimensional ablation coefficient, depends on the species parameter and is determined by solving the gas dynamic equations for the ablation flow for each set of (n_e, T_e, r_p). A function fitting these results is used in M3D-C[1]. X_m is the usual law used for strongly shielded cryogenic pellets. The granule radius r_p and thus the source width decreases as the granule is ablated by the plasma, as $\delta r_p/\delta t = -C\ (n_e, T_e, r_p) \times X_p$. More details on the model can be found in [10][11].

3. Results

The simulations presented in this paper start from experimental NSTX equilibrium, electron density and temperature profiles. The target plasma is an ELMy H-mode (plasma discharge 129015) [6] with reliable temperature measurements during the inter-ELM period. The main parameters are $B_T = 0.44$ T, $I_p = 0.785$ MA, a = 0.627 m. The simulation is initiated at 0.4 s from the beginning of the discharge, within an inter-ELM time interval. The separatrix is at R = 1.48 m and the top of the pressure pedestal is at R = 1.46 m at that moment (see Figure 2). A series of simulations were performed of injections with different radius, initial speed, injection angle and size of the ablation cloud, as summarized in table 1:

r_p (in mm)	Inj. Velocity (in m/s)	Source width (in cm)	Inj. angle (in degree)
0.2 – 1	50 – 200	1 - 5	-75 to +75

Typical meshes sizes are 1 - 5 mm and the time step is $10^{-8} – 10^{-7}$ seconds.
Overall, it takes between 0.2 and 3 milliseconds for the pellet to totally ablate, which is consistent with experimental values [7]. Comparing to previous L-mode simulations [12], the penetration depth and the ablation time is up to one order of magnitude shorter due to the higher electron density and temperature in H-mode. In these simulations, the granule starts propagating inward at R = 1.5 m with a constant velocity. When entering the plasma, the granules generate a large and localized density increase as can be seen in Figure 1.

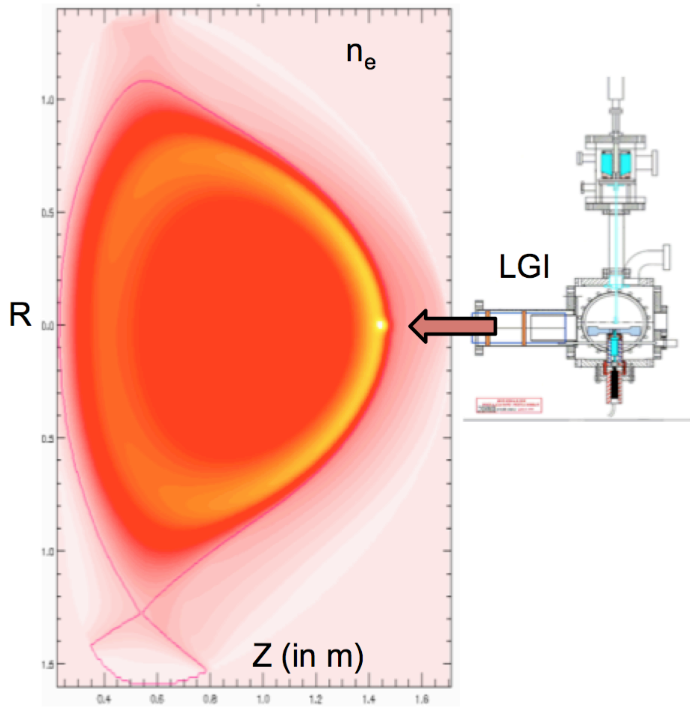

FIG. 1. Poloidal cross-section of the density contours. The increase is due to the injection of a 0.8 mm granule in NSTX.

On a short timescale, electron conduction along the field lines reheats this high-density region and leads to a localized plasma pressure increase. An example of pressure increase due to the injection of a 0.8 mm granule is shown in Figure 2. A pressure increase is also found in the Scrape-Of-Layer (SOL), which is associated to the boundary conditions used in the open field lines region, which are keeping the temperature constant even when the density increases.

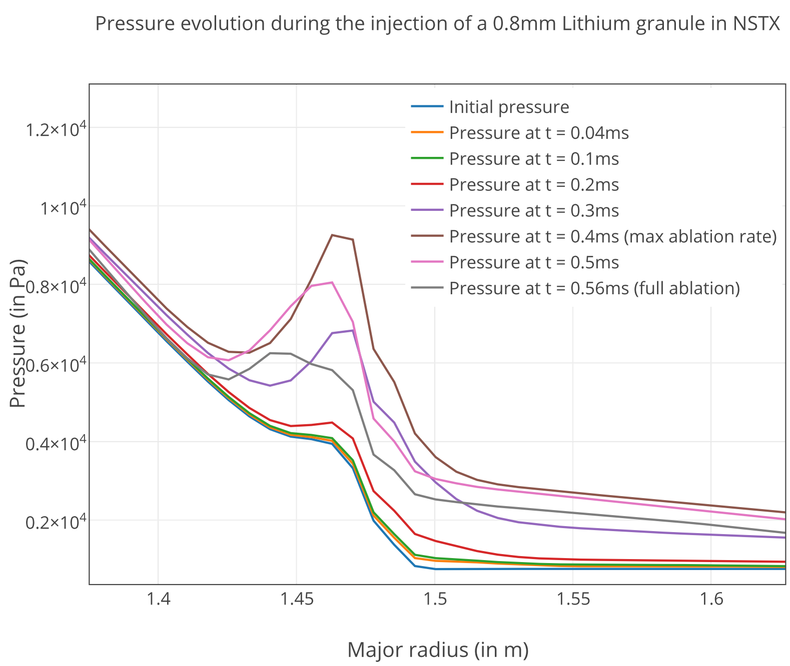

FIG. 2. Successive pressure profiles at the poloidal plan where the granule is injected. A large increase of the pedestal pressure is observed.

Figure 3 shows the number of ablated atoms injected in the simulations. The larger granules achieve a significantly larger penetration depth, up to 7 cm for 1 mm granules at 100 m/s, i.e. 3 cm inside the pedestal top. Figure 3 also shows that while the number of particles locally deposited at the pedestal top is higher for large granules, they also inject a large number of particles inside the separatrix. The associated pressure increase at maximum ablation is shown on Figure 4, showing that the larger the granule is, the larger the increase of the pressure gradient is.

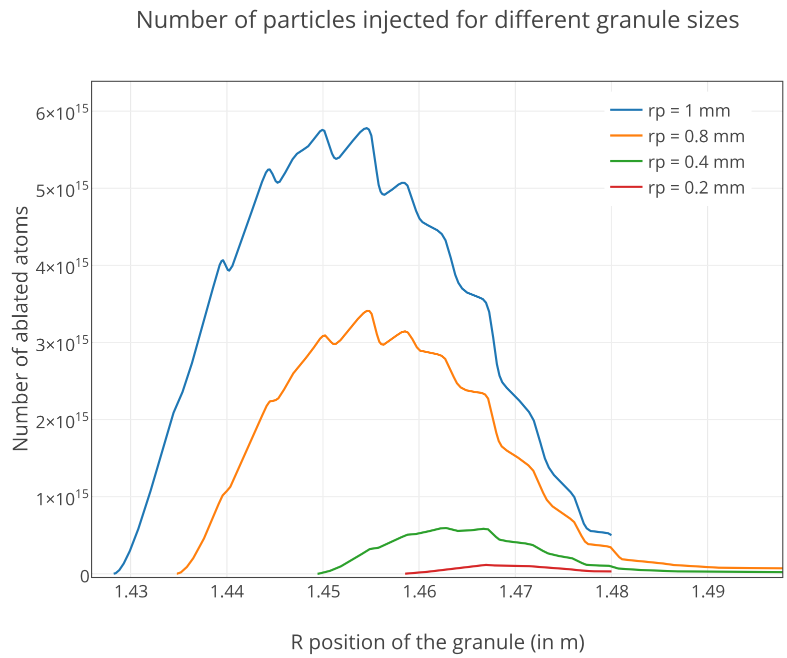

FIG. 3. Number of ablated atoms injected as the granule is penetrating into the plasma. The top of Pressure pedestal is at R = 1.46 m for this NSTX discharge, and the seperatrix at R = 1.48 m.

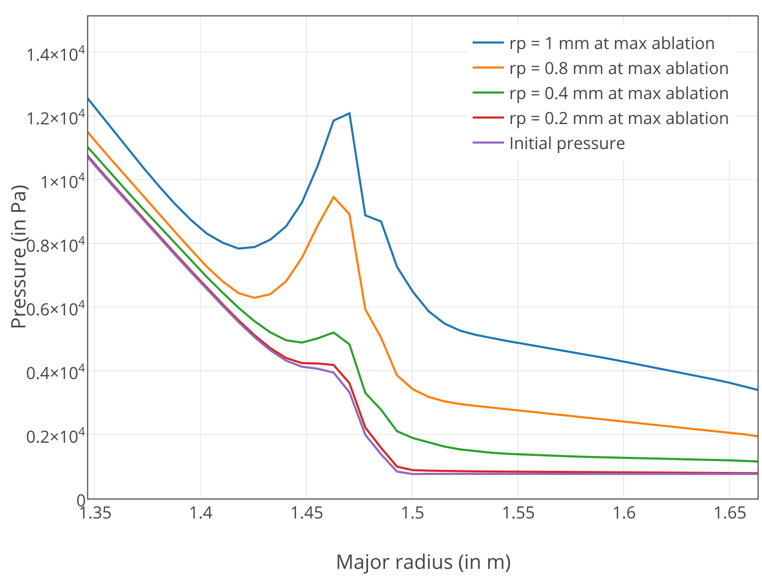

FIG. 4. Pressure profile at maximum ablation for different granule sizes

The initial velocity at which the granule is injected also changes the penetration depth and particle deposition as can be seen on Figure 5. For this particular case, slower granules deposit more particles at the pedestal top and also lead to a smaller fueling. The associated pressure increase at maximum ablation is presented on Figure 6 and shows that the pressure perturbation is lower for the fast granules compared to the slower ones. Note here that these are qualitative results, as the current model does not include effects arising from the non-uniformity of the magnetic field, which may decelerate the granule. These effects will be included and tested in future work.

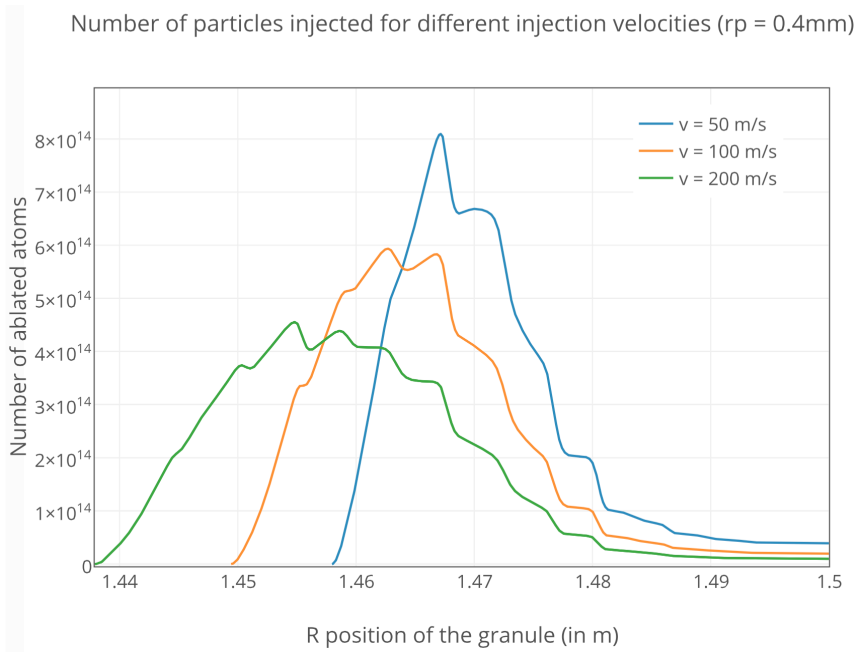

FIG. 5. Number of ablated atoms injected when the granule is penetrating into the plasma. Injection of a 0.4 mm granule with different velocities. The top of the pressure pedestal is at R = 1.46 m for this NSTX discharge.

Simulations with injections of a 1 mm granule in NSTX H-mode with varying angles of injection have been done. No significant differences have been observed between upward and downward injections and injecting with an angle α with a velocity V_{inj} is also very similar to injecting with no angle at a velocity of $\cos(\alpha) \times V_{inj}$.

Finally, the impact of the size of the ablation cloud has been tested. Three simulations have been done, injecting granules of the same size (i.e. same number of particles and ablation rate) but with a wider source, i.e. larger ablation cloud. The lower value (1 cm) is determined by numerical limitations of the current grid. In our simulations, the density increase is larger for small width sources but within the range tested (1-5cm) it has a small impact (few %) on the maximum induced pressure perturbation. Note that it is the radial width of the source which is varied here. The effect of the toroidal width of the source has been tested in recent 3D simulations and has shown a more significant impact. These simulations start from the same NSTX equilibrium and the same number of particles injected. They typically include 16 to 32 toroidal planes. The toroidal localization of the source is varied from a quasi-axisymmetric source to one with a toroidal width of 120 degrees. The localized density and pressure increase is larger as the source toroidal width decreases.

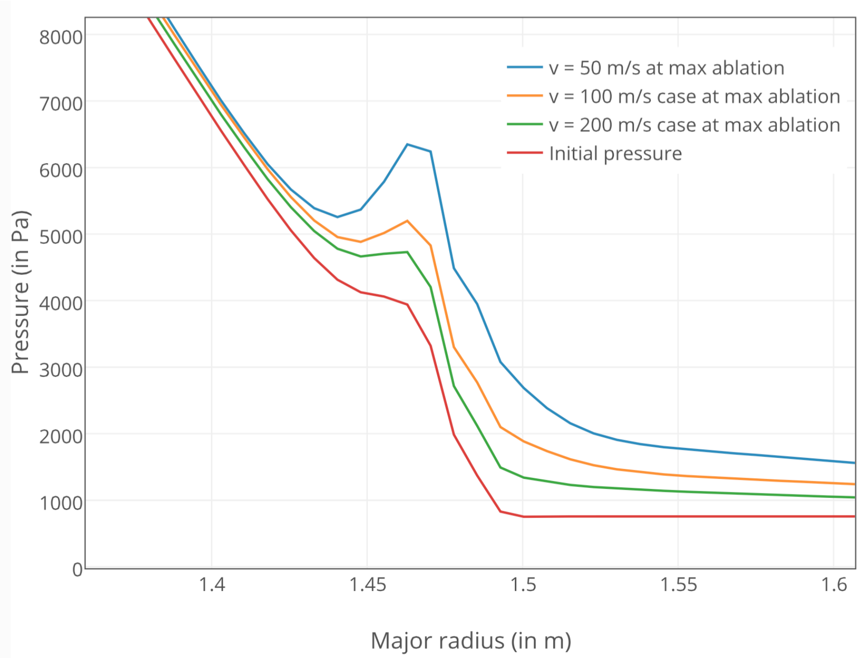

FIG. 6. Pressure profiles for different injection velocities (at maximum ablation).

Toroidal harmonics up to n = 8 have been included in these simulations and high-order modes are quickly destabilized right after the Li injection. The magnetic energy amplitude increases as the source width decreases, i.e. the pressure localized peaking, as can be seen on Figure 7. The dominant modes are n=1 and n=4. Figure 8 shows the pressure perturbation induced by the lithium injection in this NSTX 3D case. Current memory limitations on Princeton clusters prevent us from modeling further this case and to reach the highly localized sources that are presumably required to trigger ELMs. Current priority is thus to reproduce these simulations on the Cori cluster (NERSC) with higher poloidal and toroidal resolutions.

4. Discussion and perspectives

These simulations show that the local pressure perturbation at the pedestal induced by LGI increases with granule size and decreases with velocity. To avoid an undesirable decrease of the temperature inside the separatrix, one can inject granules with a larger injection angle or by decreasing the injection velocity. An LGI system has been installed on NSTX-U and synthetic diagnostics (line integrated measurement of density from interferometry, heat-flux footprint in vicinity of the strike-points) are currently being implemented in M3D-C[1]. This will allow a comparison of the predicted density increase at the edge to the measured values.
Granules with a high injection velocity are not found to be always beneficial. A fast granule might increase the pedestal pressure gradient very quickly, but to values below the ELM-triggering threshold, when slower granules might increase the pedestal gradient above this threshold for the same number of injected particles. 3D simulations are on going to specify quantitatively this threshold and the impact of granule parameters on ELM properties. These simulations aim at finding an effective compromise between fast ELM-pacing and high confinement. Preliminary 3D simulations already show the impact of the toroidal localization of the density source on the amplitude of the magnetic energy, in particular for high-order modes. Current effort aims at further decreasing the source toroidal localization via mesh packing techniques and adaptive meshing.

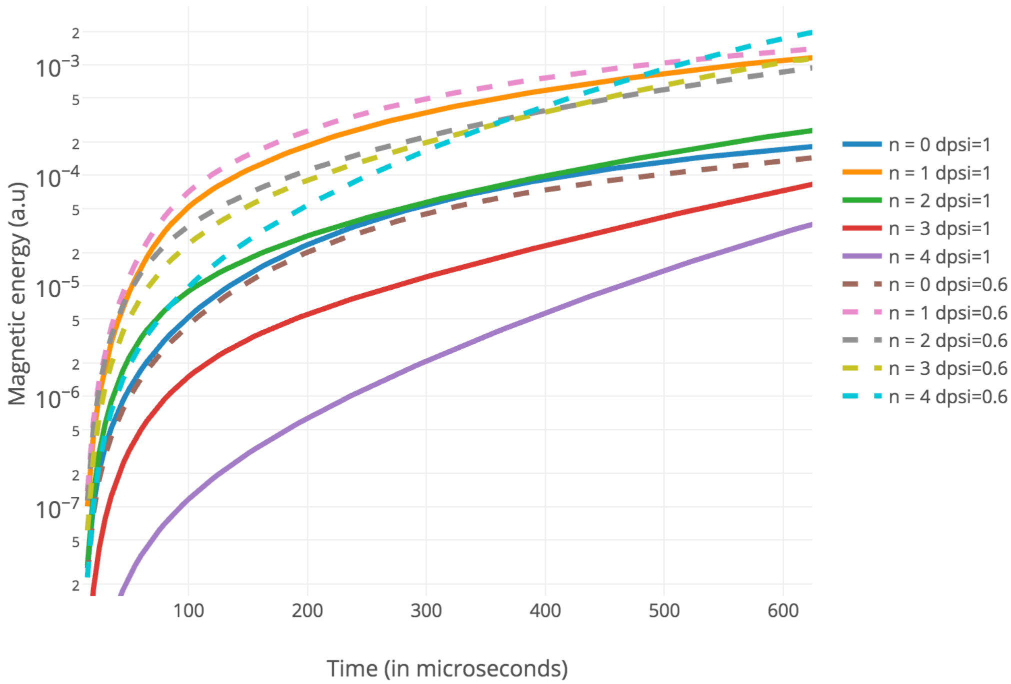

FIG. 7. Magnetic energies of harmonics n = 0-8 for 3D simulations of LGI in a NSTX H-Mode plasma. Only the toroidal width of the source is varied between the two simulations.

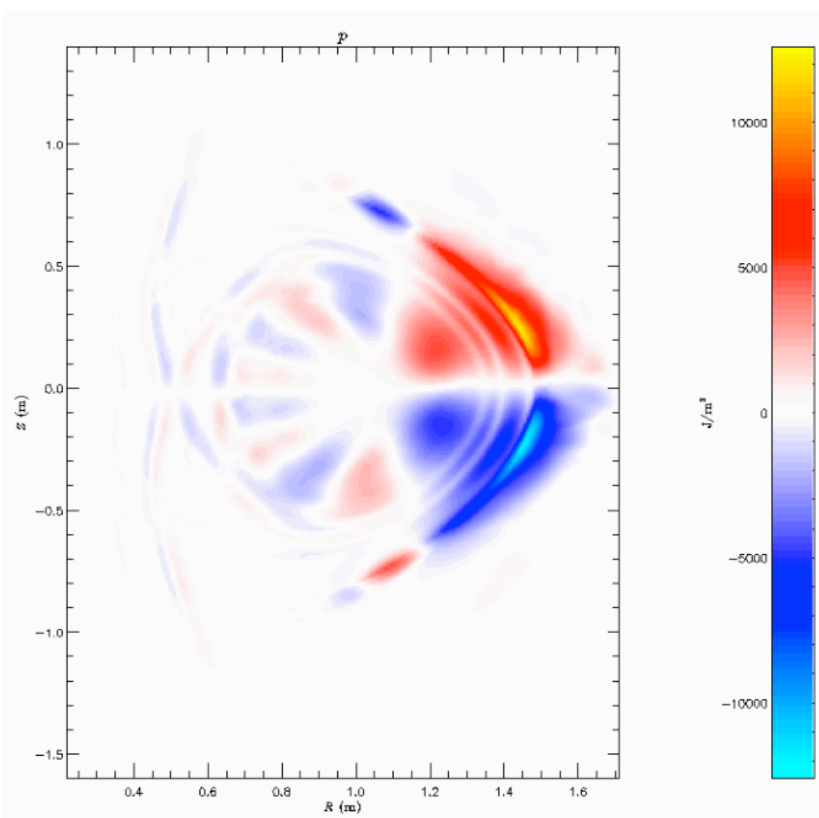

FIG. 8. Pressure perturbation at $t = 80\ \tau_A$ after a lithium injection in NSTX (3D case with 16 poloidal planes).

Acknowledgments. This manuscript is based upon work supported by the U.S. Department of Energy, Office of Science, Office of Fusion Energy Sciences, and has been authored by Princeton University under Contract Number DE-AC02-09CH11466 with the U.S. Department of Energy. The publisher, by accepting the article for publication acknowledges, that the United States Government retains a non-exclusive, paid-up, irrevocable, worldwide license to publish or reproduce the published form of this manuscript, or allow others to do so, for United States Government purposes.

[1] S.C. JARDIN, et al., Computational Science & Discovery, 5 (2012) 014002

[2] R. NAZIKIAN, et al., Proceedings of IAEA 2014, EX1-1

[3] R.J. HAWRYLUK, et al., Nucl. Fusion 55 (2015) 053001

[4] D. K. MANSFIELD, et al., Nucl. Fusion 53 (2013) 113023

[5] W. M. SOLOMON, et al., PRL 113, 135001 (2014)

[6] R. MAINGI, et al., PRL 103, 075001 (2009)

[7] A. BORTOLON, et al., Nucl. Fusion 56 (2016) 056008

[8] A. BORTOLON, et al., Proceeding of the 22nd PSI conference (2016)

[9] R. LUNSFORD, et al., Fusion Eng. Des. (2016)

[10] P. B. PARKS, et al., Nuclear Fusion 34 417 (1994)

[11] P. B. PARKS, et al., to be published

[12] A. FIL, et al., Proceeding of the 57th Annual Meeting of the APS Division of Plasma Physics